Supporting Information

# Concentrated electrolyte boosting high-temperature cycling stability of $LiCoO_2$/graphite battery

Min Zhang[a,=], Jianjun Zhang[b,c,=,*], Jinfeng Yang[b,c,=], Jianhua Yao[b], Zheng Chen[b], Chenglong Lu[b], Xiaofan Du[b], Zhongyi Zhang[a], Hui Zhang[a,*], Guanglei Cui[b,*]

[a] *College of Material Science and Engineering, Qingdao University, No. 308 Ningxia Road, Qingdao 266071, P. R. China*

[b] *Qingdao Industrial Energy Storage Technology Institute, Qingdao Institute of Bioenergy and Bioprocess Technology, Chinese Academy of Sciences, Qingdao 266101, P. R. China*

[=] *These authors contributed equally to this work.*

Corresponding author.

*E-mail address:* zhanghui_29@163.com

zhang_jj@qibebt.ac.cn

cuigl@qibebt.ac.cn

**Experimental Section**

*1.1 Sample collection*

Lithium hexafluorophosphate ($LiPF_6$) was provided by Jiangsu Guotai Super Power New Materials Co., Ltd. Lithium difluoro(oxalato)borate (LiODFB) was purchased from Suzhou Qianmin Chemistry Co., Ltd. Ethylene carbonate (EC, 98%) and dimethyl carbonate (DMC, 99%) was supplied by Macklin. Glass fiber (thickness: 200 μm) was obtained from Whatman Company.

1.2 Sample characterizations

The viscosity of electrolytes was evaluated with a DMA 35 density meter and a Lovis 2000M viscometer, respectively. The morphologies of pristine $LiCoO_2$ cathode and cycled $LiCoO_2$ cathodes were characterized by scanning electron microscopy (SEM) (Hitachi S-4800, operating at 3 kV) and high resolution transmission electron microscopy (HR-TEM) (Tecnia G20, FEI), respectively. ESCALab220i-XL spectrometer was used to investigate the X-Ray photoelectron spectra (XPS) of graphite anode and $LiCoO_2$ cathodes disassembled from cycled $LiCoO_2$/graphite full cells at 90 ºC. Inductively coupled plasma-optical emission spectrometer (ICP-OES) was used to investigate the dissolution concentrations of cobalt (Co) ions from cycled $LiCoO_2$ cathodes using 1.0 M EC/DMC/$LiPF_6$, 0.5 M EC/DMC/LiODFB, 1.0 M EC/DMC/LiODFB and 2.0 M EC/DMC/LiODFB, respectively. $LiCoO_2$ cathodes disassembled from cycled $LiCoO_2$/graphite full cells in full charged state were soaked in EC/DMC solvent at 90 °C for 24 hrs before ICP-OES characterization.

*1.3 Electrochemical evaluation*

Ionic conductivity of the samples was tested by electrochemical impedance spectroscopy (EIS) using an Autolab PGSTAT 302N system at varied temperatures ranging from 30 ºC to 80 ºC. The samples were sandwiched between two stainless-steel plate electrodes. The DC conductivity (σ) was obtained using the formula:

$$\sigma = \frac{L}{S \times R}$$

Here, S and L are the contact area and thickness of glass-fiber separator filled with electrolyte, respectively. R is the electrolyte resistance. Electrolyte resistance (R) is obtained from a Nyquist plot, which is tested by electrochemical impedance spectra

(EIS) with a frequency ranging from 1 Hz to $10^6$ Hz with an AC amplitude of 10 mV. The electrochemical stability of the samples was measure by linear sweep voltammetry (LSV) from 0 to 6 V with a sweep rate of 1 mV $s^{-1}$ for lithium/ stainless-steel cells assembled with four different electrolytes at 25 $^oC$.

The $LiCoO_2$ cathode was composed of 95 wt. % $LiCoO_2$ power, 3 wt. % PVDF/NMP binder and 2 wt. % carbon black. Areal density of obtained $LiCoO_2$ cathode was 12.75 mg $cm^{-2}$. The graphite anode was composed of 94 wt. % graphite power, 6 wt. % LA133 binder. The $LiCoO_2$/graphite full cells were charged and discharged between 2.75 V − 4.2 V at a wide temperature range (25 $^oC$, 90 $^oC$, −5 $^oC$ and −15 $^oC$) on a LAND battery testing system (CT2001A, Wuhan LAND electronics Co., Ltd.) (1 C=130 mA $g^{-1}$). The cells assembly were carried out in an argon filled glove box, with oxygen content less than 2 ppm and $H_2O$ content less than 1 ppm. The impedance and polarization evaluations of $LiCoO_2$/graphite full cells using different electrolytes after different cycles were compared by electrochemical impedance spectroscopy (EIS) in the frequency range from 10 mHz to 7 MHz.

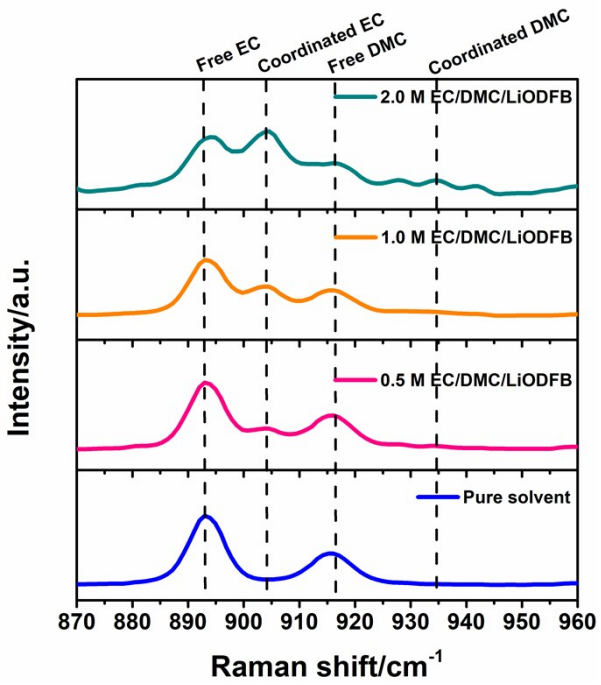


**Fig. S1.** Raman spectra of different EC/DMC/LiODFB electrolytes and pure solvent ((EC: DMC), 1:1 by volume) in the range of 870-960 $cm^{-1}$.

Raman spectra is used to study the solvation structures of electrolytes as shown in **Fig. S1**. The Raman shifts located at about 893 and 916 $cm^{-1}$ are ascribed to the stretching vibration bands of the C–O of free EC and free DMC, respectively.[1] When the LiODFB concentration increase from 0.5 M to 2.0 M, new Raman shifts are assigned to $Li^+$-coordinated EC and $Li^+$-coordinated DMC appear at 904, 934 $cm^{-1}$, respectively.[1] In addition, the relative intensities of these new peaks increase, while the intensities of the peaks of free EC and free DMC decrease with the increase of LiODFB concentration. Above results indicate that more EC and DMC molecules participate in $Li^+$ solvation.

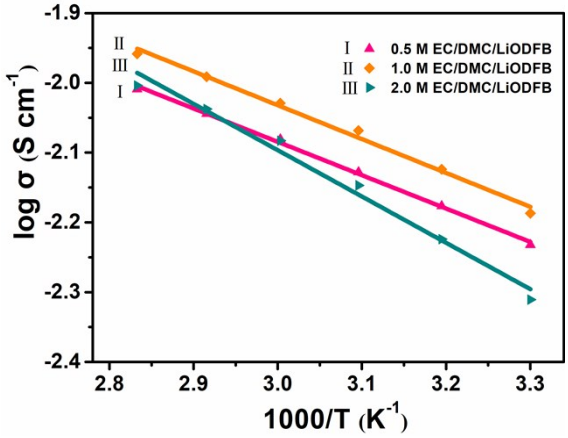


**Fig. S2.** Ionic conductivity of stainless steel/stainless steel symmetrical coin cells using 0.5 M EC/DMC/LiODFB, 1.0 M EC/DMC/LiODFB and 2.0 M EC/DMC/LiODFB at different temperatures.

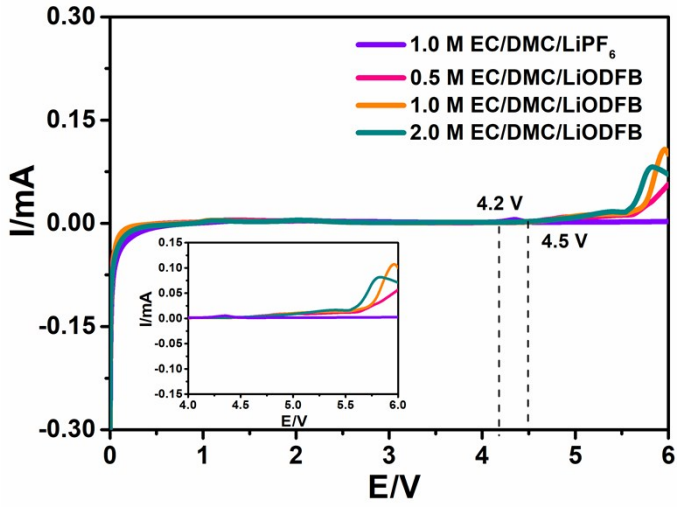


**Fig. S3.** Linear sweep voltammetry (LSV) of stainless steel/Li asymmetrical coin cells using 1.0 M EC/DMC/$LiPF_6$, 0.5 M EC/DMC/LiODFB, 1.0 M EC/DMC/LiODFB and 2.0 M EC/DMC/LiODFB.

Ionic conductivity and electrochemical window are the parameters to rate Li ions migration ability and high voltage durability of electrolyte [2, 3]. Therefore, ionic conductivity and electrochemical window of four electrolytes are compared. As shown in **Fig. S2** and **Table S1**. 1.0 M EC/DMC/LiODFB electrolyte has the highest ionic conductivity whether at 80 °C or at 30 °C. Compared with 1.0 M

EC/DMC/LiODFB electrolyte and 0.5 M EC/DMC/LiODFB electrolyte, 2.0 M EC/DMC/LiODFB electrolyte possesses relatively lower ionic conductivity of 4.89 × $10^{-3}$ S/cm at 30 °C due to its higher viscosity. As shown in **Fig. S3**, the oxidation current starts at 4.5 V, indicating that 2.0 M EC/DMC/LiODFB electrolyte does not decompose at a voltage under 4.5 V. Therefore, this concentrated electrolyte is suitable for high voltage LIBs.

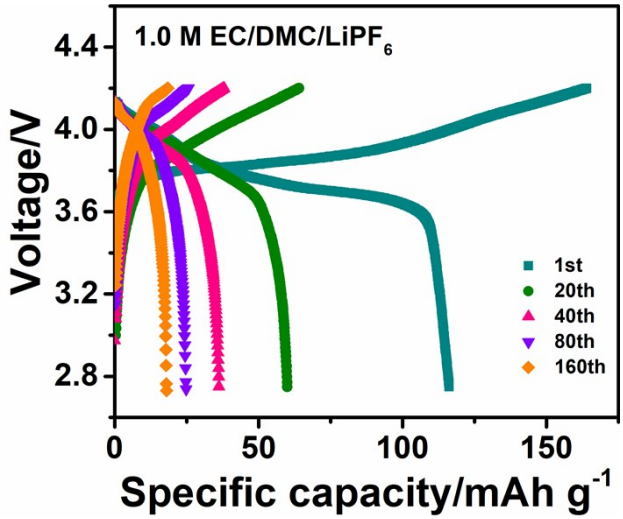


**Fig. S4.** The representative charge/discharge curves of $LiCoO_2$/graphite full cell using 1.0 M EC/DMC/$LiPF_6$ at 90 °C.

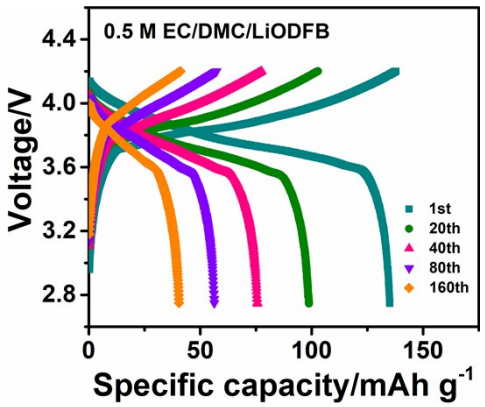


**Fig. S5.** The representative charge/discharge curves of $LiCoO_2$/graphite full cell using 0.5 M EC/DMC/LiODFB at 90 °C.

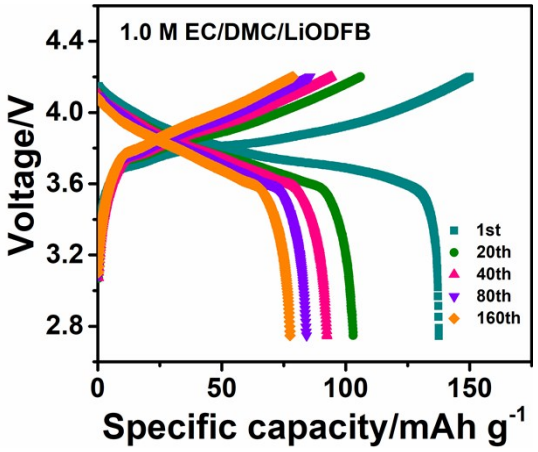


**Fig. S6.** The representative charge/discharge curves of $LiCoO_2$/graphite full cell using 1.0 M EC/DMC/LiODFB at 90 °C.

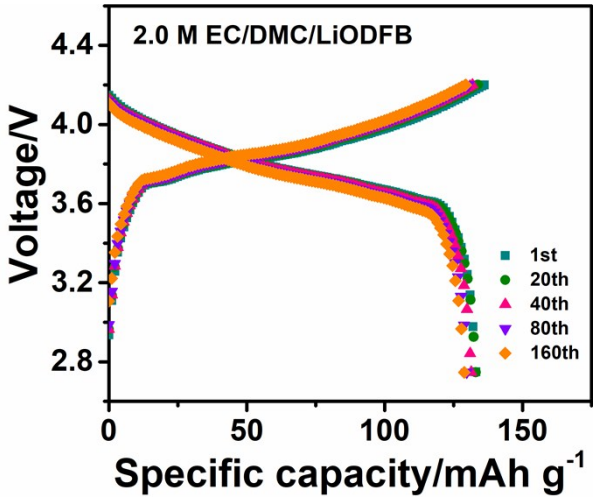


**Fig. S7.** The representative charge/discharge curves of $LiCoO_2$/graphite full cell using 2.0 M EC/DMC/LiODFB at 90 °C.

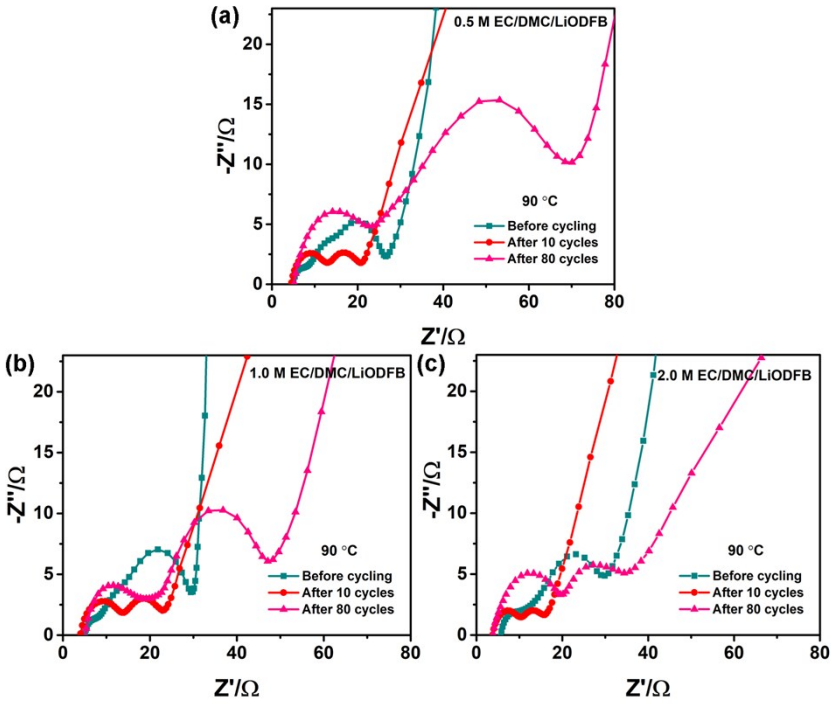


**Fig. S8.** Nyquist plots of $LiCoO_2$/graphite full cells using 0.5 M EC/DMC/LiODFB, 1.0 M EC/DMC/LiODFB and 2.0 M EC/DMC/LiODFB before cycling and after 10, 80 cycle at 90 °C.

In an effort to further disclosing the essential law of the excellent cell performance at 90 °C, AC impedance spectra of the $LiCoO_2$/graphite full cells using 0.5 M EC/DMC/LiODFB, 1.0 M EC/DMC/LiODFB and 2.0 M EC/DMC/LiODFB is analyzed before cycling, after 10, 80 cycles and shown in **Fig. S8**. It is found that there are two obvious semicircles in the impedance spectra of the batteries, which can be respectively assigned to interphase impedance ($R_{SEI}$) and electron transfer impedance ($R_{ct}$).[4] Apparently, all electrochemical impedances of cells using 0.5 M EC/DMC/LiODFB, 1.0 M EC/DMC/LiODFB and 2.0 M EC/DMC/LiODFB after 10 cycles at 90 °C were lower than those of before cycling, which might due to accelerated reaction dynamics and thermodynamic processes at 90 °C. In addition, both $R_{SEI}$ and $R_{ct}$ of cells using different electrolytes increased with the increase in the cycle number. This was probably because the decomposition by-products of electrolyte on the surface of electrode were poor electron conductors during the cycling.[5] The battery assembled with 2.0 M EC/DMC/LiODFB after 80 cycles shows

smallest $R_{SEI}$ + $R_{ct}$ (31 Ω) than the ones using 0.5 M EC/DMC/LiODFB (64 Ω) and 1.0 M EC/DMC/LiODFB (42 Ω).

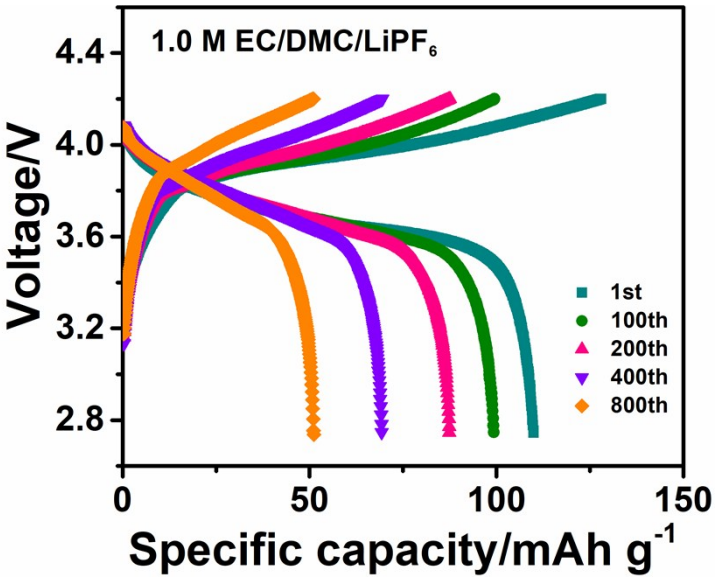


**Fig. S9.** The representative charge/discharge curves of $LiCoO_2$/graphite full cell using 1.0 M EC/DMC/ $LiPF_6$ at 25 °C.

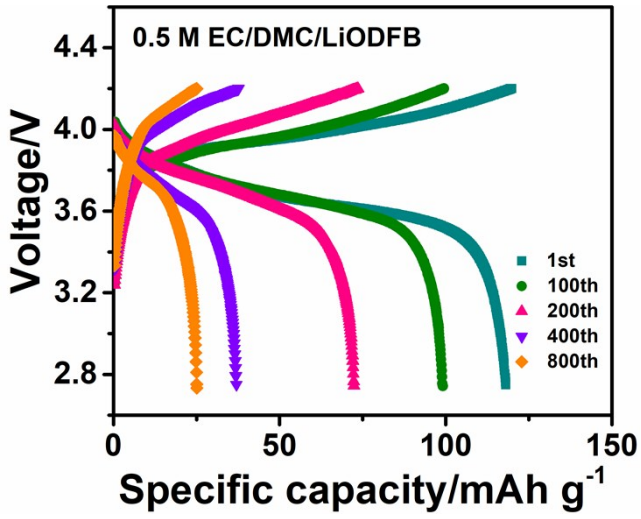


**Fig. S10.** The representative charge/discharge curves of $LiCoO_2$/graphite full cell using 0.5 M EC/DMC/LiODFB at 25 °C.

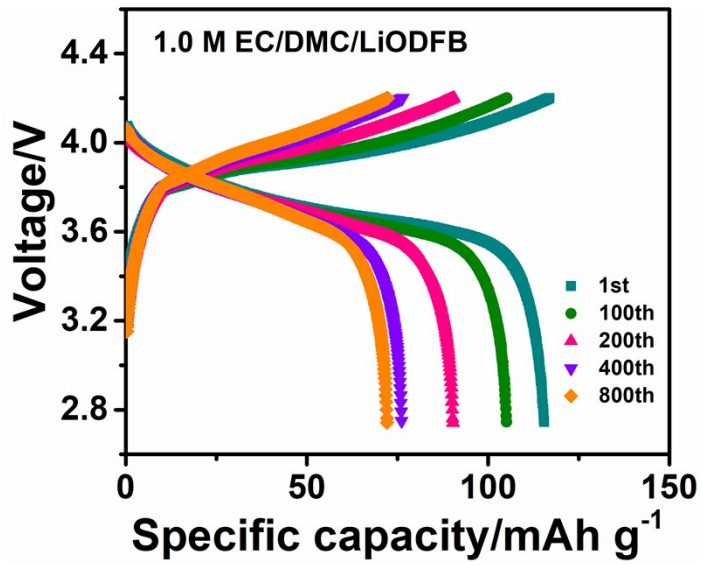


**Fig. S11.** The representative charge/discharge curves of $LiCoO_2$/graphite full cell using 1.0 M EC/DMC/LiODFB at 25 °C.

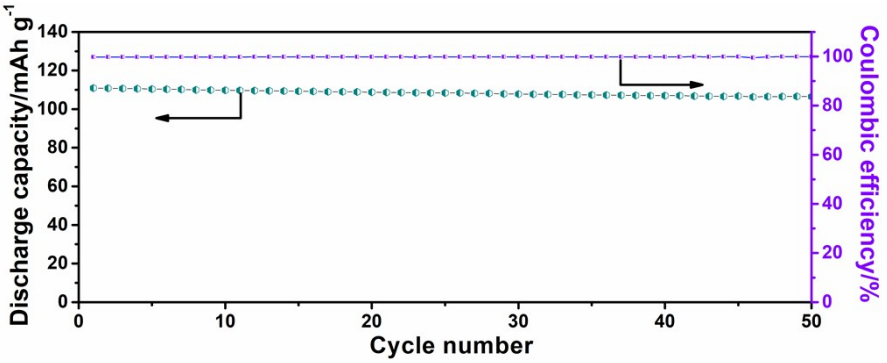


**Fig. S12.** Retention of discharge capacities at 0.1 C of $LiCoO_2$/graphite full cells using 2.0 M EC/DMC/LiODFB at −5 °C.

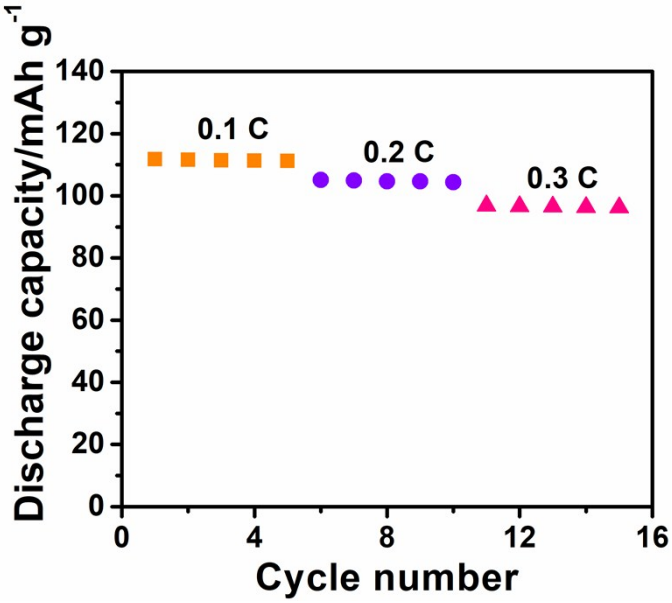


**Fig. S13.** Rate capacities of the $LiCoO_2$/graphite full cells using 2.0 M EC/DMC/LiODFB at various current densities (−5 °C).

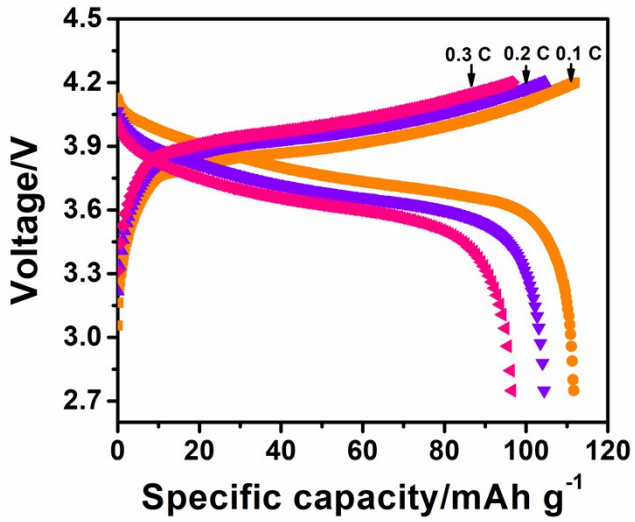


**Fig. S14.** Corresponding charge/discharge curves of $LiCoO_2$/graphite full cell using 2.0 M EC/DMC/LiODFB at 0.1 C, 0.2 C and 0.3 C. (−5 °C).

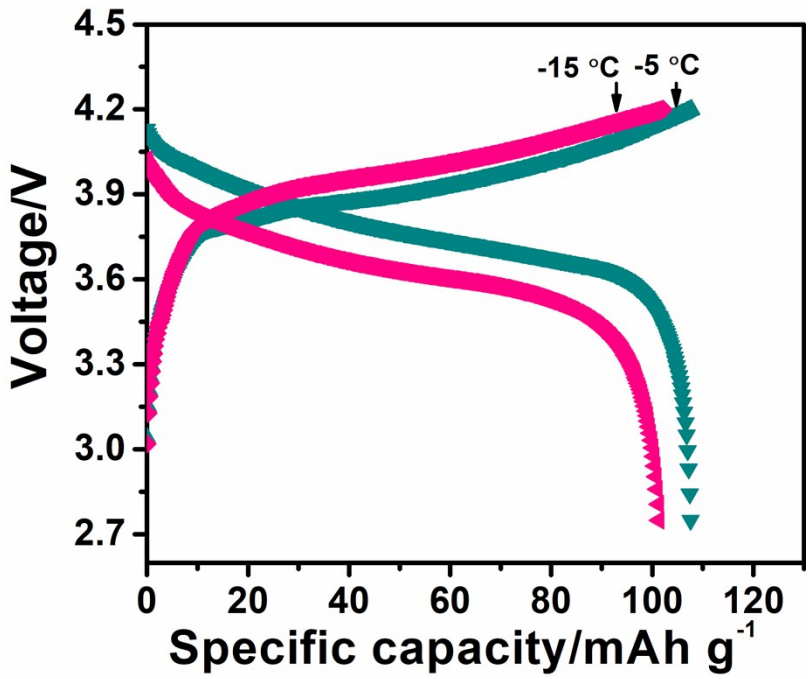


**Fig. S15.** Charge/discharge curves of the $LiCoO_2$/graphite full cells using 2.0 M EC/DMC/LiODFB at different temperatures (−5 °C and −15 °C).

Apart from long-term cycling lifespan of LIBs at ambient temperature and high temperature, the normal operation of batteries at subzero temperature is also highly vital for their actual use. At low temperature conditions, the bottleneck of LIBs is the insufficient ionic conductivity resulted from freezed electrolyte. Here, $LiCoO_2$/graphite full cells applying 2.0 M EC/DMC/LiODFB electrolyte can be directly charged-discharged at −5 °C. As can be seen in **Fig. S12**, after 50 cycles at 0.1 C rate, the discharge capacity retention of $LiCoO_2$/graphite full cells is 96% (106.5 mAh $g^{-1}$/110.9mAh $g^{-1}$) with an ultrahigh average Coulombic efficiency of 99.9%. In order to deeply investigate the low temperature performance of 2.0 M EC/DMC/LiODFB electrolyte based $LiCoO_2$/graphite full cells, discharge/charge measurements were carried out at various current densities from 0.1 C to 0.3 C with five cycles performed at each current density. The discharge capacities and the corresponding charge/discharge curves of 2.0 M EC/DMC/LiODFB electrolyte based $LiCoO_2$/graphite full cells are shown in **Fig. S13** and **Fig. S14**, respectively. When the discharge current densities increased from 0.1 to 0.3 C, the discharge capacity of cells continuously decreases because of the polarization effect which makes charge plateau

rising and discharge plateau declining. At a current density of 0.1 C, 2.0 M EC/DMC/LiODFB electrolyte based $LiCoO_2$/graphite full cell has a discharge capacity of 111.9 mAh $g^{-1}$. Even at a current density of 0.3 C, the discharge capacity still reaches 96.5 mAh $g^{-1}$.

More encouragingly, at an extreme low temperature of −15 °C, $LiCoO_2$/graphite full cell can still be directly charged–discharged using 2.0 M EC/DMC/LiODFB electrolyte (**Fig. S15**). Additionally, this cell still demonstrates an admirable capability of discharging (101.3 mAh/g shown in **Fig. S15** at −15 ºC, which is as close to 88% as that of at 25 ºC (115.6 mAh/g shown in **Fig. S7**). This fully indicates that this concentrated electrolyte could enable $LiCoO_2$/graphite battery excellent charge-discharge performance at subzero temperature.

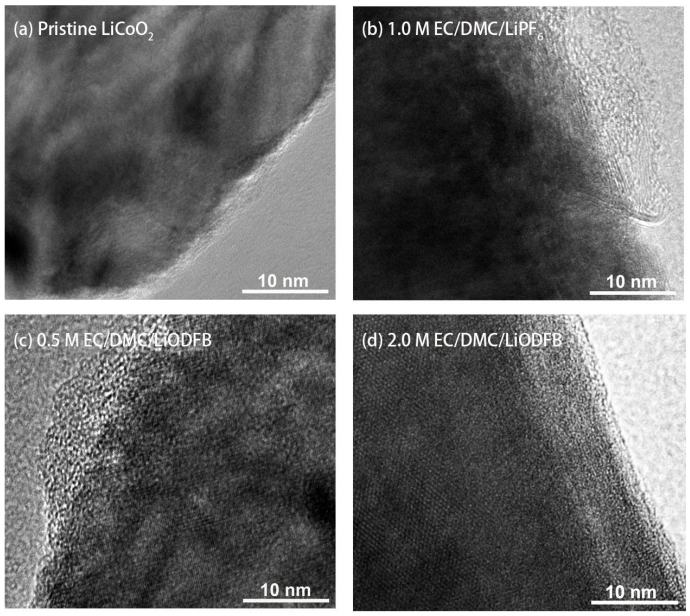


**Fig. S16.** HR-TEM images of (a) pristine $LiCoO_2$ cathode and cycled $LiCoO_2$ cathodes disassembled from $LiCoO_2$/graphite batteries after 160 cycles using (b) 1.0 M EC/DMC/$LiPF_6$, (c) 0.5 M EC/DMC/LiODFB and (d) 2.0 M EC/DMC/LiODFB at 90 ºC, respectively.

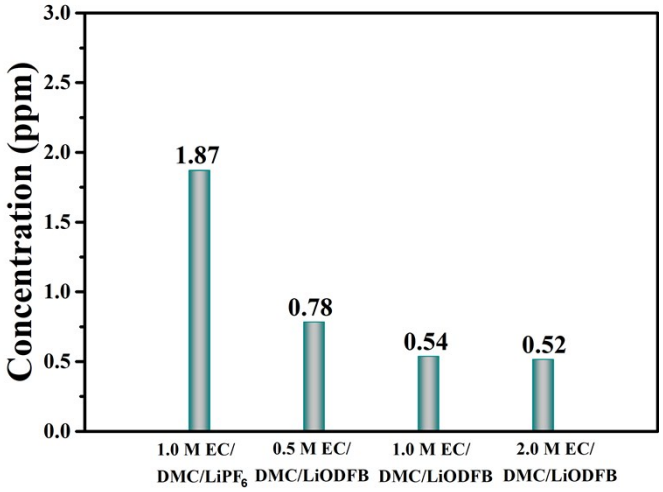


**Fig. S17.** ICP-OES results of dissolution concentrations of cobalt (Co) ions from cycled $LiCoO_2$ cathodes using 1.0 M EC/DMC/$LiPF_6$, 0.5 M EC/DMC/LiODFB, 1.0 M EC/DMC/LiODFB and 2.0 M EC/DMC/LiODFB at 90 ºC, respectively.

**Fig. S17** presents the dissolving of cobalt ion of cycled $LiCoO_2$ cathodes with different electrolytes dissembled from disassembled from $LiCoO_2$/graphite battery after 160 cycles at 90 ºC. Higher Co ion contents from cycled $LiCoO_2$ cathodes using 1.0 M EC/DMC/$LiPF_6$ (1.87 ppm), 0.5 M EC/DMC/LiODFB (0.78 ppm) and 1.0 M EC/DMC/LiODFB (0.54 ppm) are detected, while the Co ion content from that using 2.0 M EC/DMC/LiODFB is only 0.52 ppm. The results indirectly suggest that the compatible CEI film formed by this concentrated electrolyte can effectively inhibit the dissolution of Co element.

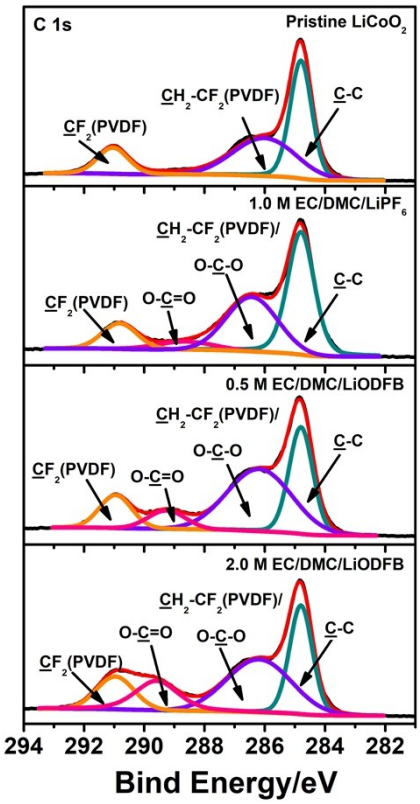


**Fig. S18.** C 1s XPS spectra of pristine $LiCoO_2$ cathode and cycled $LiCoO_2$ cathodes disassembled from $LiCoO_2$/graphite batteries after 160 cycles using 1.0 M EC/DMC/$LiPF_6$, 0.5 M EC/DMC/LiODFB and 2.0 M EC/DMC/LiODFB at 90 ºC, respectively.

As depicted in the **Fig. S18**, the pristine one contains three major peaks at C 1s spectrum: a peak at 284.8 eV is assigned to C-C bond of conductive carbon in the LiCoO2 cathode, other two peaks are assigned to the polyvinylidene fluoride (PVDF) binder. After cycling, new peaks of O-C-O (≈ 286.2 eV in C 1s), O-C=O (≈ 289.2 eV in C 1s) emerge on both cycled cathodes due to the deposits of electrolyte component decomposition.

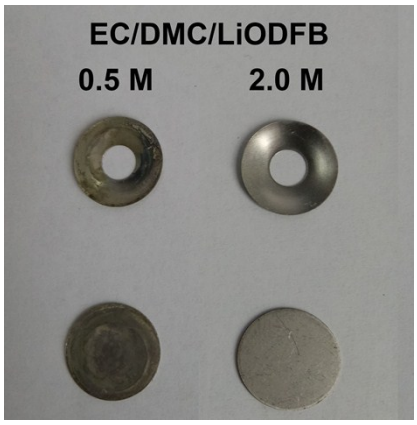


**Fig. S19.** Digital photographs of contact elastic plates and stainless-steel plates retrieved from $LiCoO_2$/graphite full batteries after 160 cycles using 0.5 M EC/DMC/LiODFB and 2.0 M EC/DMC/LiODFB at 90 ºC, respectively.

**Fig. S19** compares the contact elastic plates and stainless-steel plates retrieved from cycled $LiCoO_2$/graphite full cells using 0.5 M EC/DMC/LiODFB and 2.0 M EC/DMC/LiODFB electrolyte. Both the contact elastic plate and stainless-steel plate disassembled from cycled $LiCoO_2$/graphite full cells using 2.0 M EC/DMC/LiODFB electrolyte still maintain the metallic luster while those of 0.5 M EC/DMC/LiODFB electrolyte turn black due to the decomposition of electrolyte.

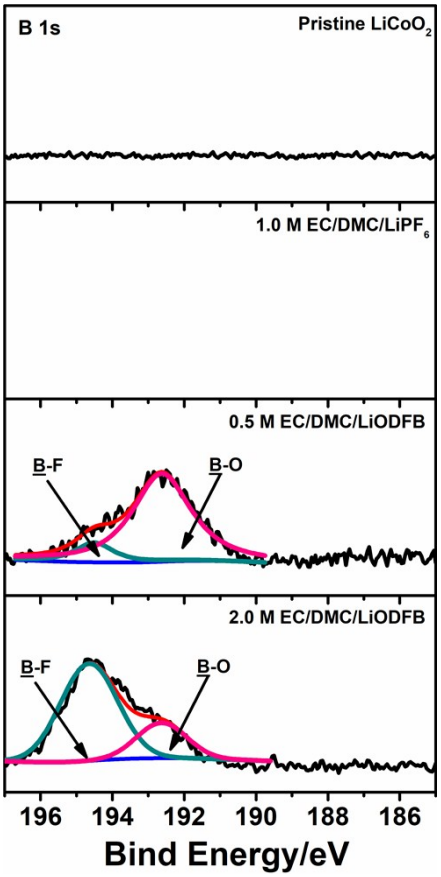


**Fig. S20.** B 1s XPS spectra of pristine $LiCoO_2$ cathode and cycled $LiCoO_2$ cathodes disassembled from $LiCoO_2$/graphite batteries after 160 cycles using 1.0 M EC/DMC/$LiPF_6$, 0.5 M EC/DMC/LiODFB and 2.0 M EC/DMC/LiODFB at 90 ºC, respectively.

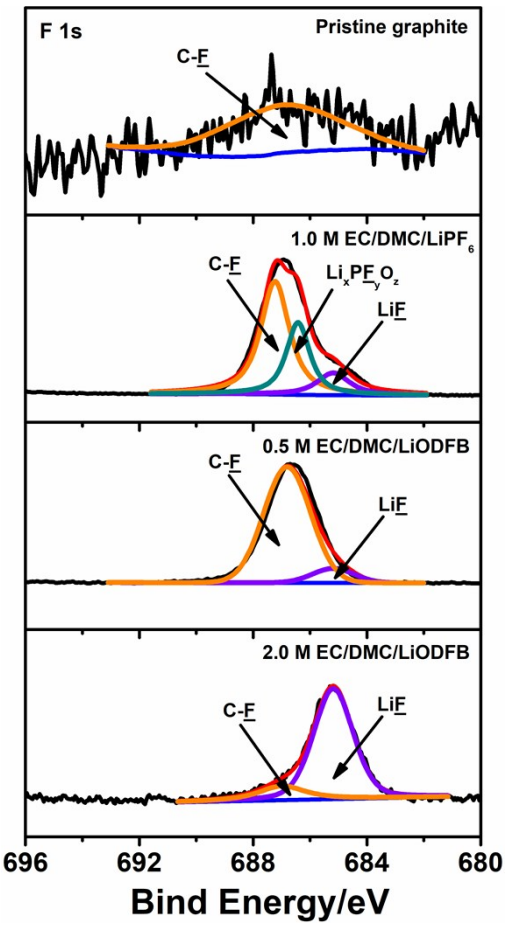


**Fig. S21.** F 1s XPS spectra of pristine graphite anode and cycled graphite anodes disassembled from $LiCoO_2$/graphite full cells using 1.0 M EC/DMC/$LiPF_6$, 0.5 M EC/DMC/LiODFB and 2.0 M EC/DMC/LiODFB after 160 cycles 90 ºC, respectively.

Compared with F 1s spectra of cycled graphite disassembled from $LiCoO_2$/graphite full cell using 1.0 M EC/DMC/$LiPF_6$ and 0.5 M EC/DMC/LiODFB electrolyte, there is an increased relative content of LiF (≈ 685.18 eV) in that of 2.0 M EC/DMC/LiODFB electrolyte (see **Fig. S21**). LiF resulted from the reduction of lithium salts is a normal component of interface layer. It is reported that the LiF-enhanced interface layer not only has better adhesion to the electrode surface, but also is a thinner and much robuster protective layer with enhanced thermal stability and mechanical property[6,7]. The result suggest that this concentrated electrolyte may contribute to the formation of a compact interface film on the $LiCoO_2$ cathode by shifting from a solvent decomposition to a salt anion decomposition.

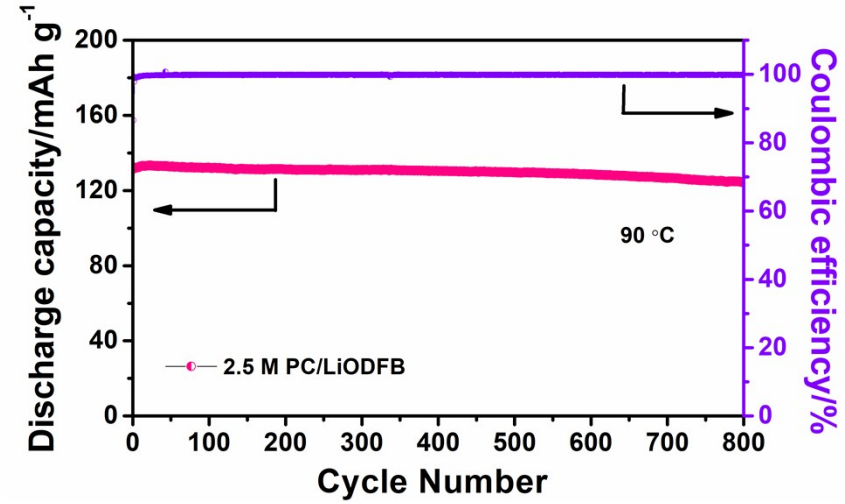


**Fig. S22.** Cycle performance (1 C) of $LiCoO_2$/graphite full cell using 2.5 M PC/LiODFB at 90 °C.

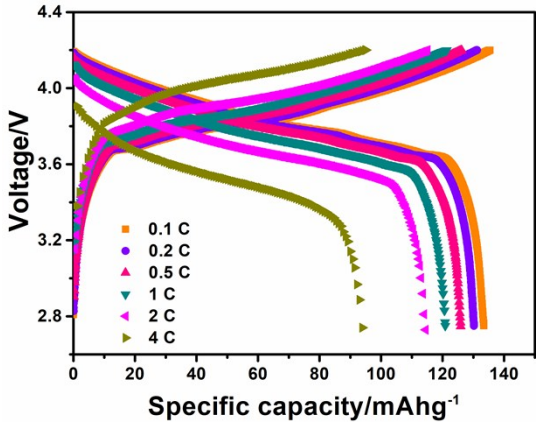


**Fig. S23.** Rate capability of $LiCoO_2$/graphite full cell using 2.5 M PC/LiODFB at 90 °C.

**Table S1.** Ionic conductivity of 0.5 M EC/DMC/LiODFB, 1.0 M EC/DMC/LiODFB and 2.0 M EC/DMC/LiODFB at 30 °C and 80 °C.

| Electrolytes | Ionic conductivity (S/cm) (30 °C) | Ionic conductivity (S/cm) (80 °C) |
|---|---|---|
| 0.5 M EC/DMC/LiODFB | $5.86 \times 10^{-3}$ | $9.79 \times 10^{-3}$ |
| 1.0 M EC/DMC/LiODFB | $6.50 \times 10^{-3}$ | $1.10 \times 10^{-2}$ |
| 2.0 M EC/DMC/LiODFB | $4.89 \times 10^{-3}$ | $9.91 \times 10^{-3}$ |

**References**


1 M. Morita, Y. Asai, N. Yoshimoto, *J. Chem. Soc. Faraday T.*, 1998, **94**, 3451.

2 J. Zhang, L. Yue, P. Hu, Z. Liu, B. Qin, B. Zhang, Q. Wang, G. Ding, C. Zhang, X. Zhou, J. Yao, G. Cui, L, *Sci. Rep.*, 2014, **4**, 6472.

3 W. Zhou, H. Gao, J. B. Goodenough, *Adv. Energy Mater.*, 2015, **6**, n/a.

4 T. T. Dong, J. J. Zhang, G. J. Xu, J. C. Chai, H. P. Du, *Energ. Environ. Sci.*, 2018, **11**, 1197.

5 J. Liu, A. Manthiram, *Chem. Mater.*, 2009, **21**, 1695.

6 A. Lahiri, N. Borisenko, A. Borodin, M. Olschewski, F. Endres, *Phys. Chem. Chem. Phys.*, 2016, **18**, 5630.

7 Y. Lu, Z. Tu, L. A. Archer, *Nat. Mater.*, 2014, **13**, 961.